

PPS020-01

Room:103

Time:May 24 08:30-08:45

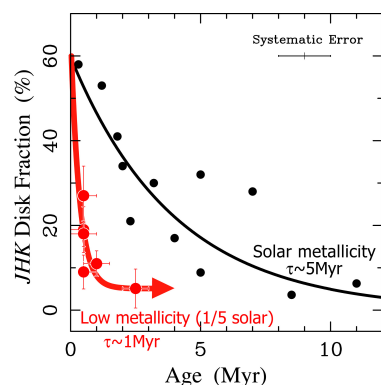
The Lifetime of Protoplanetary Disks in Low-metallicity Environments

Chikako Yasui^{1*}, Naoto Kobayashi², Masao Saito¹, Alan T. Tokunaga³, Chihiro Tokoku⁴

¹NAOJ, ²Institute of Astronomy, Univ. of Tokyo, ³IfA, Univ. of Hawaii, ⁴Univ. of Tohoku

Although as many as over 500 exoplanets are now known, these planets are unexpectedly found to be diverse in terms of, e.g., mass, orbital period, and eccentricity. Perhaps the most telling discovery in exoplanet study is the "planet-metallicity correlation," the higher probability of a star hosting a giant planet with increasing metallicity, suggesting that metallicity could be the most crucial parameter for giant planet formation.

We studied near-infrared disk fractions of six young clusters in the low-metallicity environments ($\sim 1/10$ solar metallicity) using deep JHK images with Subaru 8.2 m telescope. We found that disk fraction of the low-metallicity clusters declines rapidly in < 1 Myr, which is much faster than the ~ 5 -7 Myr observed for the solar-metallicity clusters (see Figure), suggesting that disk lifetime shortens with decreasing metallicity possibly with an $\sim 10^Z$ dependence. Since the shorter disk lifetime reduces the time available for planet formation, this could be one of the major reasons for the strong planet-metallicity correlation. Although more quantitative observational and theoretical assessments are necessary, our results present the first direct observational evidence that can contribute to explaining the planet-metallicity correlation.



Keywords: protoplanetary disk, metallicity, disk dispersal, exoplanet

PPS020-02

Room:103

Time:May 24 08:45-09:00

Evolution of the size of dust grains by evaporation and condensation

Takuto Kuroiwa¹, Sin-iti Sirono^{1*}

¹Earth & Environmental Sci. Nagoya Univ.

1. Background

The coagulations of dust grains of sub micron size which have silicate cores covered by ice mantle form the dust aggregates with high porosities in the outer protoplanetary disk in the initial phase of the planet formation. Whether dust grains grow up by coagulations in initial phase affects the planet formation materially.

On the other hand, the previous experiments indicate that the chondrules in meteorites were formed by temporal heating and cooling. If temporal heating events which increase the temperature to 10^3 K occurred in the disks, temporal heating events which increase the temperature to 10^2 K such that the ice evaporates often occurred. Thus, we consider that dust grains experience the evaporation and the condensation through the temporal heating events

We consider that H_2O gas molecules condense on the surface of dust grains through the decreasing temperature in the temporal heating event. In this process, the dust grains are covered by the ice in this process to grow up for the ice mantle thickening. Then the larger size of dust grains has the lower saturation pressure of water vapor than smaller by the effect of the surface tension for sub-micron size of dust grains. Thus, the larger dust grains become larger by condensation. This process changes the size distribution of dust grains. The size development of the dust grains affects collision velocity and static adhesion, and changes the mechanical property of the dust aggregates.

2. Purpose

We calculate the time development of the probability distribution function for the size of dust grains through the temporal heating event by the numerical simulation.

3. Results

We calculate at 3AU from the central star in typical disk. We set the initial time at the time of beginning the condensation and that initial distribution function for the size of dust grains is proportional to power law -3.5 of size (Mathis et al. 1977). We calculate in the range of cooling rates from 10^6 Kh^{-1} to 10^2 Kh^{-1} . The results indicate that the growth phase bisects and time evolution of size is stopped. In the stopped time, the size distribution of the dust grains becomes the bipolar distribution of many small dust grains of silicate and a few large dust grains covered by the ice.

We divide the growth phase between the first phase and the second phase. In the first phase, the larger dust grains become larger from the largest dust grains by the condensation for the decrease of saturation pressures of water vapor of dust grains by the temperature. On the other hand, the decrease of the pressure of surrounding water vapor by the condensation catches up with the decrease of the saturation pressures to decide the minimum size covered by the ice. Next phase is the second phase. In this phase, the transferring H_2O molecules among smaller dust grains and larger dust grains works because the decrease of the surrounding pressure is larger than the decrease of the saturation pressures of dust grains. The transferring effect evolves small dust grains covered by the ice into smaller dust grains. In the case, dust grains once developed become initial size by the evaporation. Finally, few surrounding H_2O gas molecules by the condensation and the lower temperature stop the size development. The distribution of dust grains becomes the bipolar distribution of a few larger dust grains and many smaller dust grains. We discuss possible effects of the bipolar distribution to the planet formation.

Keywords: dust grain, evaporation, condensation

PPS020-03

Room:103

Time:May 24 09:00-09:15

Dust particle growth and fragmentation in the dust layer with a weak turbulence

Taku Takeuchi^{1*}, Takayuki Muto¹

¹Tokyo Institute of Technology

I studied dust sedimentation and formation of the midplane dust layer at the first stage of planet formation. I assume that the gas disk is initially in a state of laminar flow. When the dust settles at the midplane and the dust-to-gas ratio there exceeds a certain value, the dust layer becomes turbulent because of the velocity difference from the upper gas layer. The strength of the turbulence is estimated from the gravitational energy liberated as the dust particles accrete toward the star. For single-sized particles with the stopping time of 0.1 Kepler time, the turbulent strength is estimated such that the alpha parameter is of the order of 10^{-6} - 10^{-5} . Under such a weak turbulence, sedimentation of the dust particles results in a strong concentration of the dust at the midplane. Consequently, in the dust layer, the gas drag effect weakens, and the radial drift velocity and mutual collision velocity of the dust particles become small. If the average dust-to-gas ratio of the whole disk is similar to the solar abundance value, the particle collision velocity does not become extremely small. For disks with the dust-to-gas ratio as large as several times the solar value, however, the maximum collision velocity cannot exceed 10 m/s. Thus, we expect that icy dust particles do not experience violent collisional destruction. I solved the coagulation equation of dust particles taking the fragmentation effect into account, and showed that icy dust particles can overcome the so-called "fragmentation barrier" if the initial dust-to-gas ratio is large enough.

Keywords: Protoplanetary disks, Dust, Planet formation

PPS020-04

Room:103

Time:May 24 09:15-09:30

Coagulation and radial drift of dust aggregates: the effect of porosity evolution

Satoshi Okuzumi^{1*}

¹Department of Physics, Nagoya Univ., ²ILTS, Hokkaido Univ.

Coagulation of dust grains is the first step towards planetesimal formation. A major obstacle is radial inward drift of macroscopic dust aggregates due to frictional coupling between gas and dust. Previous studies have predicted that the radial drift of meter-sized compact solid bodies is faster than their local collisional growth, suggesting a difficulty of direct collisional formation of planetesimals.

In this talk, we discuss how this picture can be altered by considering porosity evolution of dust aggregates. Recent laboratory and numerical experiments have revealed that dust grains evolve into highly porous aggregates as they experience low-energy collisions. The porosity evolution is important because porous aggregates have a large collisional cross section and hence a short growth timescale. We have for the first time simulated coagulation and radial drift of dust aggregates properly taking into account fractal evolution at low collisional velocities (Okuzumi et al. 2009) and collisional compression at higher velocities (Suyama et al. 2008). We find that macroscopic aggregates maintain a low internal density (typically $\sim 10^{-4}$ g/cc) in spite of the occurrence of the compression and are thus resistive to the radial infall. We plan to report this result and discuss an expected planetesimal formation scenario.

Keywords: dust aggregate, planetesimal formation, porosity evolution, radial drift

PPS020-05

Room:103

Time:May 24 09:30-09:45

The calculation of ionization degree in planetary gaseous disks: the effect of charged dust grains

Yuri Fujii^{1*}, Satoshi Okuzumi¹, Shu-ichiro Inutsuka¹

¹Nagoya University

There are many studies on the ionization degree of the protoplanetary disks, but no one has calculated that of circumplanetary disks with dust grains yet. It is important to understand the structure and evolution of circumplanetary disks, since the mass accretion through the disk onto the central planet is important in the early formation phase of the disks, and in addition, they are the sites of satellite formation. Despite the low temperature, the circumplanetary disks are ionized weakly because of galactic cosmic rays and radionuclides. Resultant ionized particles make secondary ions and molecules, and they are captured by dust grains. Weak ionization of the disk has important consequence for their evolution since the coupling between magnetic field and gas produces turbulence driven by magnetorotational instability. Thus, it is important to investigate the ionization fractions of various particles in the circumplanetary disk.

Inclusion of the effect of dust grains is essential when we calculate the ionization fraction, because the capturing of charged particles by dust grains makes the ionization degree lower. In the circumplanetary disks, dynamical timescales are shorter than that of protoplanetary disks, and timescales of various reactions are even shorter than the dynamical timescale of disks, which suggests the importance of accurate time-dependent calculation of ionization degree in disks. However, it remains difficult to calculate highly time-dependent ionization degree numerically. Okuzumi (2009) has shown that the charge distribution of dust grains can be approximated by a normal distribution. That approximation decreases the number of equations, and makes us calculate the ionized degree more quickly.

In this presentation, I will describe the important ionization processes and our fast method for calculation of charge state distributions of various particles and dust grains.

Keywords: protoplanetary disk, circumplanetary disk, ionization degree, dust grain, magnetorotational instability, numerical simulation

PPS020-06

Room:103

Time:May 24 09:45-10:00

On the Interaction between a Protoplanetary Disk and a Planet in an Eccentric Orbit

Takayuki Muto^{1*}, Taku Takeuchi¹, Shigeru Ida¹

¹Tokyo Institute of Technology

The number of planets discovered so far has exceeded 500, and approximately 200 of them have eccentricity more than 0.2. If such planets are born in a disk environment, it is important to study how they interact with the disk and how the orbital parameters of such eccentric planets evolve. In this talk, we present a new analytic approach to the disk-planet interaction that is especially useful for planets with eccentricity larger than the disk aspect ratio. In the study of disk-planet interaction conducted so far, the eccentricity of the planet is assumed to be small, and the planet orbit is decomposed into the power series of eccentricity. In this work, we make use of the dynamical friction formula to calculate the force exerted on the planet by the disk, and the force is averaged over the period of the planet. The advantage of this approach is that it is possible to apply this formulation to arbitrary large eccentricity. The resulting migration and eccentricity damping timescale agrees very well with the previous works when eccentricity is of the order of 0.2-0.5. If the planet eccentricity is close to the order of the unity, the orbital evolution timescale behaves very differently. Moreover, we have found that the timescale of the orbital evolution depends largely on the adopted disk model in the case of highly eccentric planets. We discuss the possible implication of our results to the theory of planet formation. We also present fitting formulae for the timescale of the eccentricity and semimajor axis evolution. These formulae can be especially useful in the study of population synthesis models.

Keywords: planet formation theory, disk-planet interaction, planetary migration

PPS020-07

Room:103

Time:May 24 10:00-10:15

High-resolution simulations of giant impacts of terrestrial planets using a tree-Godunov-SPH method on GPU

Natsuki Hosono^{1*}, Hidenori Genda², Shigeru Ida¹

¹Tokyo Institute of Technology, ²The University of Tokyo

Smoothed Particle Hydrodynamics (SPH) method is a useful numerical tool in studying a number of astronomical and planetary science problems.

A wide variety of astrophysical and planetary science problems are studied by SPH method.

The giant impact hypothesis, one of the possible scenario of the Moon formation, is one of such a problem.

In order to examine the giant impact scenario for the Moon formation, numerical simulations of collisions between planetary embryo have been done by SPH method.

However, the problem that the current SPH method does not have resolution enough fine for debris disk is pointed out.

In the SPH method, the resolution is determined by the number of SPH particles.

To obtain high resolution, we must construct fast calculation code.

In this study, a procedure for construction of new fast SPH code is described.

We implement the following three improvements to the code.

First, we implement so-called Tree method to SPH.

While the direct search of neighbors and calculations of self-gravity among N particles require $\sim O(N^2)$ computations, the introduction of the tree method reduces the number of computations to $\sim O(N \log N)$.

Secondly, we implemented approximate Riemann solver to the SPH method, which is called the Godunov SPH.

The application of the Riemann solver enable us to simulate phenomena with strong shocks.

Furthermore, Godunov SPH method includes appropriate dissipation in solving shock flows.

The calculation time becomes 10 times faster than that of the standard SPH.

Finally, we write the SPH code to run the program on massively parallel Graphical Processing Units (GPU) supporting the NVIDIA CUDA architecture.

The calculation time of GPU is about $O(10)$ times faster than that of CPU.

In order to check the accuracy and performance of this code, we perform two types of benchmark tests.

One is the model of the adiabatic collapse of an initially isothermal spherical gas cloud to check the performance of GPU.

We perform this test by two methods, tree Godunov SPH on GPU and tree standard SPH on CPU.

Another is the collision between planet-size objects to check the correct treatment of non-ideal EOS.

From these tests, we obtain that our code is about 300 times faster than the prevailing SPH method.

By using this code, simulations with large number of particles, namely high resolution simulations, are feasible.

In future work, to obtain further improvement of the performance of GPU, we will implement memory rearrangement algorithm.

This allows us to obtain the most efficient memory bandwidth.

Keywords: giant impact, SPH, GPU

PPS020-08

Room:103

Time:May 24 10:15-10:30

Proto-atmosphere of a giant icy satellite accreted in a gas-starved circumplanetary disk

Hidetaka Okada^{1*}, Kiyoshi Kuramoto¹

¹Hokkaido Univ.

The interiors of Ganymede, Callisto and Titan are differentiated, but the mechanism and timing of their differentiation remain an open question.

For this problem, there are two types of theories; one assumes the differentiation during satellite accretion and another assumes that after the satellite formation.

The major heat source during satellite accretion is the accretional energy by planetesimal collision. If ice component supplied from planetesimal evaporates by the accretional energy, it is possible that a proto-atmosphere form. In that case, the blanketing effect of proto-atmosphere raises the satellite surface temperature higher than that of the case without proto-atmosphere. If the blanketing effect is so strong as to melt ice component, the internal differentiation is possibly induced.

Pioneering studies about the proto-atmosphere of giant icy satellite during accretion are Lunine and Stevenson (1982) and Kuramoto and Matsui (1994). For environment of satellite accretion, the former assumed satellite formation in a thick circumplanetary disk, and the latter assumed that in vacuum. According to the most recent theory widely accepted, satellite may have accreted in a gas-starved circumplanetary disk (Canup and Ward, 2002, 2006). This model points out the internal differentiation of giant icy satellite does not take place during accretion because the accretion timescale is estimated to be longer than that in previous studies. However, this diagnostic is based on the model analysis of a steam proto-atmosphere assuming gas-free accretion and neglects the effect of surrounding disk gas. The properties of proto-atmosphere composed of mixed gas from the disk and ice evaporant may be significantly different from those of previous atmospheric models.

In this study, we have estimated the radiative-convective equilibrium structure of a proto-atmosphere connected with a thin gas disk hydrostatically, and calculated the satellite surface temperature as a function of satellite size and accretional energy flux. We then attempt to clarify the condition for internal differentiation of giant icy satellite accreted in a gas-starved circumplanetary disk.

As a preliminary calculation, radiative-convective equilibrium structures are solved for the present sized Ganymede embedded within the disk gas with temperature and pressure of 180 K and 12 Pa, respectively, given thermal energy fluxes at the satellites surface. When the thermal energy flux exceeds 300 W / m^2 , the total optical depth for infrared radiation exceeds 1 mainly because of absorption by H_2O vapor in the proto-atmosphere. In this case, strong blanketing effect emerges and thereby the surface temperature becomes higher than the melting point of H_2O . Such value of thermal energy flux is equivalent to that of the accretional energy flux when Ganymede is accreted for time slightly shorter than 10^6 yr.

As the thermal energy flux is larger than about 600 W / m^2 , the position of tropopause locates beyond the radius of the gravitational sphere of satellite. In this case, it is expected that proto-atmosphere enriched in H_2O vapor flows out into surrounding disk. The similar result is obtained by Kuramoto and Matsui (1994) for gas-free accretion model, however, this study confirms that atmospheric outflow is possible even when surrounding nebula gas exists.

Japan Geoscience Union Meeting 2011

(May 22-27 2011 at Makuhari, Chiba, Japan)

©2011. Japan Geoscience Union. All Rights Reserved.



PPS020-09

Room:103

Time:May 24 10:45-11:00

An effect of adiabatic compressibility on mantle convection within super-Earths

Chihiro Tachinami^{1*}, Masaki Ogawa², Hiroki Senshu³, Shigeru Ida¹

¹Tokyo Institute of Technology, ²University of Tokyo, ³Chiba Institute of Technology

see Japanese version

PPS020-10

Room:103

Time:May 24 11:00-11:15

Magma ocean cooling and hydrodynamic escape under steam atmosphere

Keiko Hamano^{1*}, Yutaka Abe¹, Hidenori Genda¹

¹The University of Tokyo

The current planet formation theory suggests that giant impacts would have marked the final stage of terrestrial planet formation. The large amount of energy released in the giant impact event would have melted a significant part of the terrestrial planet, forming a deep magma ocean. The magma ocean would begin to cool and solidify just after the impact and its cooling time affects the differentiation of the mantle and the timing of subsequent water ocean formation.

The magma ocean cooling rate especially in the early stage should have been controlled by the radiation from the top of the atmosphere into space. It is expected that the cooling rate of the magma ocean strongly depends on the amount of the potent greenhouse gases such as water vapor and carbon dioxide. On the other hand, the amount of the gases could be controlled through the exchange between the atmosphere and the magma ocean because of their high solubility in magma. Since the melt fraction in the magma ocean decreases with its cooling, more water and carbon dioxide would be degassed into the atmosphere, which in turn leads to reduce the cooling rate. This means that the evolution of the magma ocean should have been coupled with the atmospheric growth through the volatile exchange between both reservoirs.

Elkins-Tanton (2008) calculated the time scale of the magma ocean on Earth and Mars considering the water and carbon dioxide exchange. The results suggest that the magma ocean cooling time would be at most 5 Myr even in the case of the high-volatile contents. Although the atmospheric blanketing effect was considered in terms of the heat balance on the surface, the atmospheric structure was not calculated for the cooling rate of the magma ocean in her model. Moreover, the effect of condensation of water was not included. Since the water vapor is condensable, the atmosphere would start to be saturated from its top with the cooling. In general, the outgoing radiation decreases with the cooling of the planetary surface. In the optically thick and water-saturated atmosphere, however, the outgoing radiation has a lower limit. This is because the temperature structure at the optical depth of unity is independent on the surface temperature in such an atmosphere. It is expected that whether or not the solar insolation exceeds the radiation limit would make a significant difference in the thermal history of the magma ocean.

If the insolation exceeds the radiation limit, the outgoing radiation could balance with the insolation. In this case, the hot steam atmosphere may persist for a long time so that the significant amount of water could be lost by hydrodynamic escape of hydrogen. The solar UV radiation dissociates water vapor into hydrogen and oxygen atoms in the upper atmosphere. Some previous studies suggest that the strong EUV from the young Sun could drive hydrodynamic loss of hydrogen, while that oxygen could be left behind because of its heavier atomic weight. If the oxygen accumulates into the atmosphere, this would cause the slowdown in the hydrogen escape. During the magma ocean stage, however, such an accumulation would not happen because the oxygen left in the atmosphere behind would be absorbed to oxidize the magma at the surface. This significant water loss also would affect the magma ocean cooling.

We developed a simple coupled atmosphere-magma-ocean model to calculate the magma ocean cooling time under steam atmosphere and the amount of water at the end of solidification, taking into account the water loss by hydrodynamic escape. We used a 1D radiative-convective equilibrium model of condensable gray gas atmosphere. The temperature structure was assumed to be adiabatic in the convective magma ocean. Hydrogen loss rate was given by the energy-limited escape rate. We will present the results of a parametric study on the cooling timescale and the amount of the steam atmosphere varying the orbit radius and the initial amount of water on the Earth-sized planet.

Keywords: Magma ocean, Hydrodynamic escape, Giant impact, Water, Radiation limit

PPS020-11

Room:103

Time:May 24 11:15-11:30

The amounts of liquid water when the oceans occupy half of the planet, under the local precipitation

Miyuki Wakida^{1*}, Yutaka Abe¹, Hidenori Genda¹

¹The University of Tokyo

It is more than 15 years since the first discovery of extrasolar planet, and more than 500 planets have been discovered. Most of the known exoplanets are gas giant planets like Jupiter. However, the discovery of terrestrial planets is just beginning through the improvements in observational instruments, which make us expect that some exoplanets may have life.

The presence of liquid water on the planetary surface is considered to be an important condition for habitable planets. But exoplanets with liquid water do not always have globally covered oceans like Earth. Some exoplanets may have a small amount of liquid water on their surface as the lakes, which may be also habitable.

Abe et al. (2005) considered a hypothetical planet not having topography and transportation of liquid water on its surface. Precipitation and evaporation are balanced in local on such planets. Abe et al. (2005) called them 'land planets'. Numerical experiments with 3 dimensional atmospheric general circulation model (GCM), assuming that the planet have a very little water (less than 1 meter on average), showed that liquid water localizes at high latitude and it is dry at low latitude of land planets. It is also found that the habitable zone of land planets is 3 times wider than that of planets with globally covered oceans like Earth (we call them 'aqua planets'). This is because the destabilizing effect of water on climate, (i.e., the runaway greenhouse effect and the ice albedo feedback), are both weaken on land planets.

The condition for being land planet is that the location where evaporation is higher than precipitation maintains wet owing to the transportation of liquid water on the surface. To extract a condition for distinction between land planets and aqua planets, systematic GCM experiments with various amounts of water under a lot of topographic maps are needed.

However, doing experiments with all parameters on GCM is very difficult, because the experiments using GCM take a lot of time. In this research, for preparing the experiments on GCM, we estimate the amounts of water for a distinction between land planets and aqua planets as follows. Abuku (2009) used percolation theory and showed mathematically that a condition for global covered oceans is equivalent to a condition that oceans occupy about a half of the planet, assuming that low potential area become ocean on a 2 dimensional random potential area. But on real planets, all low potential area does not always become ocean because precipitation localizes. Precipitation occurs at high latitude on land planets (Abe et al., 2005). So we made a lot of random topographic maps using planets' topographic data and poured water from north and south poles. We consider that the amounts of liquid water when oceans occupy a half of the planet is close to the amounts of liquid water for distinction between land planets and aqua planets. So we estimated the amounts of liquid water when oceans occupy a half of the planet, under various topographic maps.

PPS020-12

Room:103

Time:May 24 11:30-11:45

Effects of obliquity and carbon cycle on the multistable solutions of climate of water-rich extraterrestrial planets

Yoshiyasu Watanabe^{1*}, Eiichi Tajika², Shintaro Kadoya¹

¹Earth and Planet. Sci., Univ. of Tokyo, ²Complexity Sci. & Eng., Univ. of Tokyo

Water-rich terrestrial planets like the Earth are expected to be found in the extrasolar planetary systems in the near future. To discuss habitability of such planets, we have to investigate characteristic features of climate system of the water-rich terrestrial planets.

One of the key factors which controls climate is "obliquity", that is, the inclination of planet's axis. The climate of the Earth is stable partly because the Earth's obliquity is stabilized by the existence of the Moon, although it is not the case, in general, for other planets. Considering a large influence of obliquity on the solar energy distribution on the planetary surface, obliquity variations could induce large climate change on the planets.

In this study, we investigate the climate of the water-rich terrestrial planets systematically under various obliquities and solar flux conditions, and with a negative feedback mechanism of carbonate-silicate geochemical cycle. We use a one-dimensional energy balance climate model (1D-EBM) with a simple model of carbonate-silicate geochemical cycle in order to understand characteristic behaviors of the climate system of water-rich terrestrial planets. The main results obtained in this study are as follows;

1. We classified the behaviors of the climate system without carbonate-silicate geochemical cycle (i.e. a constant $p\text{CO}_2$ condition) into the following 4 stable solutions: 1) ice-covered solution (snowball solution), 2) seasonal ice-cap solution, 3) permanent ice-cap solution, and 4) ice-free solution. Seasonal ice-cap solution exists at lower solar flux conditions compared with ice-free solution at low obliquity, shrinking with an increase in the obliquity and disappearing at 54 degrees. Permanent ice-cap solution also exists at lower solar flux compared with seasonal-ice-cap solution at the obliquity less than 28 degrees. Above the obliquity of 54, either ice-free solution or snowball solution can exist.

2. When carbonate-silicate geochemical cycle is taken into account, the range of solar flux condition for all the solutions expand at any obliquities, indicating that the carbon cycle make the condition for habitable climate broader range of semi-major axis inside the habitable zone.

3. In the planets with carbonate-silicate geochemical cycle, we found that $p\text{CO}_2$ does not depend strongly on obliquity, even if the climate mode is different. This is because, with an increase in obliquity, a decrease of weathering rate at low latitudes may tend to be compensated by an increase of weathering rate at high latitudes.

4. Large CO_2 degassing rate could maintain warm climate even if the solar flux is lower. At low obliquity (for example, 23.4 degrees), warm climate cannot be maintained by much lower CO_2 degassing rate (for example, 0.6 times the degassing rate of the Earth today). However, at high obliquity (for example, 90 degrees), warm climate can be maintained by lower CO_2 degassing rate (for example, at most 0.3 times the degassing rate of the Earth today), compared with at small obliquity condition.

Keywords: extraterrestrial planet, planetary climate, obliquity, carbonate-silicate geochemical cycle, degassing, EBM

PPS020-13

Room:103

Time:May 24 11:45-12:00

Effects of Orbital Eccentricity on Habitability of Earth-like Extra-solar Planets with Carbon Cycle

Shintaro Kadoya^{1*}, Eiichi Tajika², Yoshiyasu Watanabe¹

¹Earth and Planetary Sci., Univ. of Tokyo, ²Complexity Sci. & Eng., Univ. of Tokyo

In this study, we systematically investigate the climate of the planets with varying orbital eccentricity and semi-major axis, and with carbonate-silicate geochemical cycle. We adopt a one-dimensional energy balance climate model and weathering model by Walker et al. (1981). We try to find conditions for the Habitable zone (HZ) of eccentric planets, and clarify the factors to determine the Habitable zone of eccentric planets. The results shows that there are three possible climate phases, namely Ice-free, Ice-cap, and Snowball phase, and nine climate modes, namely Runaway Greenhouse (RG), Ice-Free (IF), Seasonally Ice-cap (SIC), Ice-cap (IC), Seasonally Snowball/Ice-free (IF), Seasonally Snowball (SSB), Snowball (SB), Cyclic Snowball (CSB), and CO₂ Condensation (CO₂C) modes. The term 'phase' is defined here as a transient state of climate, and the term 'mode' as an annual or long-term state of climate. The HZ is consist of the regions where a planet has liquid water on its surface, i.e. IF, SIC, IC, SSI, and SSB mode. The inner boundary of IC mode and the lower boundary of SSB, which are both the limits of the HZ, are found to be determined by annual mean insolation and perihelion distance, respectively.

If the heat capacity was very large, surface temperature would be averaged over a long period. It means that the climate of the planet would be affected by the annual mean insolation. This is why the inner boundary of IC is determined by annual mean insolation because of large heat capacity of IC mode planets.

On the other hand, if the heat capacity was very small, the temperature would follow the variation of insolation instantly. It means that the variation of the distance between from the central star, i.e. the perihelion and aphelion distance, would determine the climate of the planet. This is why the lower boundary of SSB is determined by perihelion distance because of the small heat capacity of SSB mode planets.

It appears that carbonate-silicate geochemical cycle also affects on the width of the HZ due to negative feedback effect which stabilizes the climate. When carbon cycle is considered, the width of the HZ becomes broader than when it is not considered.

The eccentric planets with large semi-major axis are habitable even in the early stage of stellar evolution. On the other hand, planets with small semi-major axis withdraw from the HZ in earlier stage of stellar evolution.

We, therefore, conclude that planets with large semi-major axis and high eccentricity should to be in the HZ for a long time.

Keywords: habitability, orbital eccentricity, carbonate-silicate geochemical cycle, EBM

Japan Geoscience Union Meeting 2011

(May 22-27 2011 at Makuhari, Chiba, Japan)

©2011. Japan Geoscience Union. All Rights Reserved.



PPS020-14

Room:103

Time:May 24 12:00-12:15

Coupled macro-spin models for polarity reversals — earth, sun, and planets —

Akika Nakamichi^{1*}, Nozomi MORI², Masahiro MORIKAWA², Hideaki MOURI³, D. Schmitt⁴, A. Ferriz-Mas⁵, J. Wicht⁴

¹Koyama Astr. Obs., Kyoto Sangyo Univ., ²Ochanomizu Univ., ³Meteorological Research Institute, ⁴Max-Planck-Institut, ⁵Dept. de Fisica Aplicada, Univ. de Vigo

We propose a coupled macro-spin model to describe magnetism and its polarity reversals of the earth, the sun and the planets in this talk. This model is based on the idea that the whole dynamo mechanism is described by global interactions of many small dynamo elements. This is the minimal model to elucidate the essence of the polarity reversal dynamics described by the complicated magneto-hydrodynamics equations.

This simple model naturally yields many of the observed features of geomagnetism: its time evolution, the power spectrum, the frequency distribution of stable polarity periods, etc. In case of the earth, the dynamo element, that a macro-spin describes, is considered to be the Tayler cell in the iron fluid core produced and supported by the Coriolis force.

Keywords: geomagnetism, dynamo, scaling, coupled-spin, solar magnetism

PPS020-15

Room:103

Time:May 24 14:15-14:30

A satellite impact created Chicxulub crater

Shinichiro Mado^{1*}

¹MAROSA

1. Introduction

It is a well known hypothesis that the Chicxulub crater was created by an asteroid impact and the impact caused the extinction of dinosaurs about 65 million years ago. However, this hypothesis has difficulty to explain the extinction of dinosaurs. The most persuasive hypothesis is 'the gravity increase hypothesis'. Although only a very large scale celestial impact can explain such a great increase of the earth's gravity, but the Chicxulub asteroid is too small to increase the earth's gravity enough. Therefore, we must assume much larger celestial body impact than the Chicxulub asteroid. In truth we can explain consistently the Chicxulub crater with such a huge scale celestial impact that is enough to increase vastly the earth's gravity.

2. Difficulty in the hypothesis of the Chicxulub asteroid impact

The huge impact which created the Chicxulub crater at Yucatan peninsula about 65 million years ago, caused a global scale serious climate change that brought dinosaurs their extinction. The Chicxulub asteroid is estimated to be about 10 kilometers in diameter. However, that hypothesis has serious difficulty to explain the extinction of dinosaurs, because remained reptiles had to evolved to be dinosaurs again unless another reason to prevent them from such evolution. The most persuasive hypothesis is the gravity increase hypothesis.

3. The gravity increase hypothesis

The gravity increase hypothesis says that a sudden and large scale increase of the earth's gravity caused the extinction of dinosaurs. This hypothesis is plausible because the main feature of dinosaurs is their large body. The largest dinosaur was more than about 10 meters tall. Now the largest animal on the ground except for snakes is a giraffe which is about 5 meters tall. The tallest dinosaur was at least twice taller than the tallest animal on the ground is today. A considerable increase of the earth's gravity prevented remained reptiles from their evolution to become as large size as dinosaurs again. Except for a tremendous scale celestial impact which caused such increase in mass of the earth, no reason can explain such a large scale increase in the earth's gravity. The Chicxulub asteroid is too small to explain such a great scale increase in the earth's mass. Therefore, we must assume much greater scale celestial impact. It is plausible to think that such a great scale celestial impact must be a planetary collision between two planets of the solar system.

4. Chicxulub crater and satellites of Mars

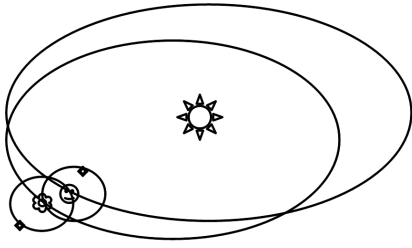
Mars has two satellites. Phobos is about 26.8 kilometers in diameter. Deimos is about 15 kilometers in diameter. The scale of martian moons are similar to the Chicxulub asteroid. Therefore, we can say that 'the Chicxulub asteroid' is a satellite of a terrestrial planet of the solar system, in its scale.

5. Conclusion

We are able to give a rational explanation to the Chicxulub crater as follows. The hitting celestial body had been a satellite of another planet. The planet also hit the old earth later and enlarged the new earth greatly. Therefore, we are able to think the Chicxulub crater to be one of proofs of the planetary collision between the old earth and the other planet of the solar system.

References

1. Thompson & Turk, (2005), "Earth Science and the Environment", Third Edition, Thomson, Brooks/Cole.
2. Faure & Mensing, (2007), "Introduction to Planetary Science: The Geological Perspective", Springer.
3. Barlow, N. G., (2008), "Mars : An Introduction to its Interior, Surface and Atmosphere", Cambridge Planetary Science, CAMBRIDGE UNIVERSITY PRESS.
4. Schlte, P., et al., (2010), 'The Chicxulub Asteroid Impact and Mass Extinction at the Cretaceous-Paleogene Boundary', "SCIENCE", Vol. 327, 5 March 2010.
5. Mado, S., (2010), 'On the Cause of the Continental Drift', "ABSTRACT Japan Geoscience Union Meeting 2010", Japan Geoscience Union.



Keywords: extinction of dinosaurs, celestial impact, planet, satellite, gravity, Chicxulub crater

PPS020-16

Room:103

Time:May 24 14:30-14:45

Formation process of ejecta morphology around the crater formed on glass beads in laboratory

Ayako Suzuki^{1*}, Toshihiko Kadono², Akiko Nakamura³, Masahiko Arakawa³, Koji Wada⁴, Satoru Yamamoto⁵

¹Center for Planetary Science, ²Inst. of Laser Engineering, Osaka Univ., ³Grad. School of Sci., Kobe Univ., ⁴PERC, Chitech, ⁵Center for Global Environ. Res., NIES

The ejecta morphologies around impact craters represent highly diverse appearance on the surface of solid bodies in our Solar System. It is considered that the ejecta morphologies depend on the emplacement processes and/or the environments when its formed, such as the atmospheric pressure, the volatile content in the subsurface, etc. Clarifying the relationships between the ejecta morphologies and formation processes/environments could constrain the ancient surface environment and the evolution of the planets.

We investigated the ejecta patterns around the impact crater which formed on a glass beads layer in laboratory, and found that the patterns depend on impact velocity, atmospheric pressure, and initial state of packing of the target [Suzuki et al., 2010, JpGU]. Now, we focus on one of the ejecta patterns which has the petal-like or concentric ridges. This ejecta pattern is very similar to so-called "rampart" morphology observed around Martian impact craters.

This series of the experiments are performed by using the two-stage light gas gun placed in Kobe University. The projectile is an aluminum cylinder, having a diameter of 10 mm and a height of 10 mm. The target is a layer of glass beads (nearly uniform diameter) in a tub with 28 cm in diameter. The bulk density is 1.7 g/cm³. The following three parameters are varied: 1) the diameter of the target glass beads (50, 100, 420 microns), 2) the ambient atmospheric pressure in the chamber (500 Pa - atmospheric pressure), 3) the impact velocity of the projectile (a few - 90 m/s).

In our experiments, the ridged patterns are observed with the condition of, 1) the diameter of the target glass beads is 50 and 100 microns, 2) the ambient pressure in the chamber is higher than 10⁴ Pa, 3) the impact velocity is higher than 16 m/s. Eventually, we succeed to capture the formation of the ridges with high-speed video camera. The ridges are formed just outside of the base of the ejecta curtain. It is found that erodible surface around the crater is essential to produce the ridges.

Keywords: Impact Experiments, Cratering, Ejecta

PPS020-17

Room:103

Time:May 24 14:45-15:00

Trial to make ramparts: Granular flow model of fluidized ejecta on Mars

Koji Wada^{1*}, Olivier S. Barnouin²

¹PERC/Chitech, ²JHU/APL

Ejecta deposits of Martian craters show evidence for extensive surface flow not typically seen at other craters on the Moon and Mercury. The exact mechanism for why such surface flow occurs remains unclear, but it must be indicating some unique surface environmental condition. Typically fluidizing agents such as water or an atmosphere have been proposed to be responsible for the formation of these deposits.

Simple granular flows can explain a wide range of flow features at landslides including their long run-out distance and lineaments, without necessarily invoking any volatiles. They might also explain fluidized deposits, with their long run-out, circumferential lineaments, thin deposit layers, and ramparts, also without necessarily invoking any volatiles or an atmosphere. In order to investigate simple granular flow models for such ejecta deposition, we use the three dimensional distinct element method (DEM). This method calculates the motion of each individual ejecta grain, taking into account mechanical interactions between grains. Our initial study showed that the surface condition is important: smooth plains with a low coefficient of friction, or readily erodible plains can produce long run-out ejecta flow (Wada & Barnouin-Jha 2006, MAPS 41, 1551). Such smooth or readily erodible Martian surfaces could be the result of sedimentary processes associated with large amounts of water that existed on Mars.

While our initial model showed that ejecta surface flow was fairly easy to achieve, it possessed too many simplifications that did not permit the formation of ramparts at the distal end of the ejecta deposits. One of the obvious simplification was that all the grains in our model were true spheres without any rolling resistance. As a consequence, grains kept rolling on flat surfaces even if the surface had a finite friction. A necessary condition to make a rampart is that the distal ejecta must stop advancing. In the DEM, this implies giving the ejecta grains rolling resistance that reflects their natural angularity. This study, thus, investigates how giving ejecta grains rolling resistance in the DEM might generate ramparts, and impact the overall emplacement and flow of granular ejecta.

In our DEM model, the mechanical interaction forces and torques between spherical grains in contact (and the floor) are expressed by the Voigt-model, which consists of a spring and dash-pot pair, in both normal and tangential directions. The spring gives elastic forces based on the Hertzian elastic contact theory. The dash-pot expresses energy dissipation during contact to realize energy dissipation with a given coefficient of restitution. For the tangential direction, a friction slider is introduced to express Coulomb's friction law with a given coefficient of friction. In this study, we introduce a rolling resistance between grains (and also the floor), which models the difficulty of rolling due to the grain angularity, expressed by a critical rolling displacement.

As an initial condition of our DEM calculations, we consider a 5-degree wedge of an ejecta curtain composed of 2958 grains with a radius of 35 m, each traveling on ballistic paths prior to deposition. This initial condition was obtained by using the ejecta scaling relationship, assuming a transient crater with a radius of ~5 km.

By introducing rolling resistance in our granular flow model, we have succeeded in stopping ejecta motion effectively. However, we have not yet succeeded in making an obvious rampart. This may be due to other simplification of our model such as the small number of grains considered, and their fairly large size. Secondary cratering of the surface material and their subsequent flow might also play a role. Further studies will explore all these factors.

Keywords: rampart, crater, Mars, granular flow, simulation, DEM

PPS020-18

Room:103

Time:May 24 15:00-15:15

Global Survey of Impact Craters on the Earth by Satellite Hyperspectral Remote Sensing

Satoru Yamamoto^{1*}, Tsuneo Matsunaga¹, Ryosuke Nakamura², Yasuhito Sekine³, Naru Hirata⁴

¹NIES, ²AIST, ³Univ. of Tokyo, ⁴Univ. of Aizu

Although more than 140 terrestrial impact craters are currently known [1], it is not clear how frequently impacts occurred in ancient Earth history. This is mainly because most of the old impact craters on the Earth are too degraded (owing to weathering and/or tectonic modification) to be identified, although intensive global survey to find impact crater structures using satellite remote sensing has not been conducted.

In this study, we try to find the traces of old impact structures on the Earth based on the visible and near infrared spectra data obtained by satellite remote sensing. Recently, the global survey using hyperspectral data by Spectral Profiler (SP) onboard SELENE/Kaguya revealed the global distribution of olivine-rich exposures on the Moon [2]. Although this global survey did not use any terrain information for the lunar surface, the location map of the detected olivine-rich spectra shows concentric distribution pattern associated with large impact structures (impact basins) on the Moon. This finding suggests that we may also find the traces of ancient impacts for even degraded impact craters on the Earth, if we focus on the distribution pattern of specific spectral features in visible and near infrared wavelength. (Here the specific spectral features do not mean the shock indicators such as Coesite and Stishovite.) If so, we can reveal the global distribution of terrestrial impact craters by satellite hyperspectral remote sensing.

To this end, it is important to understand how the terrestrial impact craters are observed in the visible and infrared spectral data by satellite remote sensing. Therefore, we examined some terrestrial impact craters, which have been identified as impact origins, using the spectral data obtained by ASTER (Advanced Spaceborne Thermal Emission and Reflection Radiometer), which is an imaging instrument with 14 bands, from the visible to the thermal infrared wavelengths, onboard NASA Terra satellite. Based on the results, we will discuss the feasibility of global survey of terrestrial impact craters by future satellite hyperspectral remote sensing.

[1] R.A.F. Grieve & E.M. Shoemaker, in Hazards due to Comets & Asteroids (T.Gehrels eds), 417-462 (Univ. of Arizona Press), 1994.

[2] S. Yamamoto, et al., Nature Geoscience, 3, No. 8, 533-536 (NGEO897) 2010.

PPS020-19

Room:103

Time:May 24 15:15-15:30

Experimental study on penetration and sticking of snow projectiles on sintered snowball

Yu-ri Shimaki^{1*}, Masahiko Arakawa²

¹Grad. School Env. Studies, Nagoya Univ., ²Grad. School Sci. Studies, Kobe Univ.

[Introduction] Icy planetesimals could be formed by collisional growth of ice dust aggregates, thus they would have an initial porosity larger than 90% [e.g., 1,2]. Since icy planetesimals are supposed to be the size of ~ 10 km, so they would have small self-gravity to cause the difficulty for re-accumulation of the fragments ejected by collisional disruption among planetesimals. Highly porous bodies such as a planetesimal would dissipate impact energy through the compression of the pores and this process allows them to stick each other. When the two bodies collide each other in sufficient different size, they could stick easily as the smaller body could penetrate into the larger body [3]. Therefore, it is expected that the initial growth of icy planetesimals is expected to be driven by direct sticking among them. In this study, we examined the impact conditions for the collisional sticking and the impact disruption of porous icy bodies; the dependencies on the porosity and the mass ratio of the projectile to the target were studied.

[Method] All impact experiments were carried out in a cold room at the temperature of -15°C in Institute of Low Temperature Science, Hokkaido University. Snow targets were made of ice particles with the average size of several 10s μm , which were prepared by spraying tiny water droplets into liquid nitrogen reservoir. These ice particles were put into a spherical mold with a constant volume, and it was gently compressed with the maximum pressure of 1 MPa. After the compression, the target was removed from the mold and it was kept in a plastic bag in order to sinter them at -15°C . All the targets had diameters of 60 mm and a porosity of 40 to 70 % (mass of 62.4 - 31.1 g), and they were sintered from 1 hour to 1 month. The projectiles were cylindrical snow with the diameter of 10 mm and the porosity of 30 % (mass of 0.35 g) sintered in 1 day at -15°C . We used three methods in order to accelerate a projectile; free fall (impact velocity of 2 - 3 m/s), spring gun (10 - 20 m/s) and He gas gun (30 - 200 m/s). The projectile was launched onto the center of the target (head on collision). The impact phenomenon was recorded by using a high-speed digital video camera with the recording rate from 1,000 - 5,000 frames per seconds and the shutter speed of 20 μs . After the impact, the mass distribution of recovered fragments was measured and the velocity distribution of the fragments was also measured. Additionally, the crater profile of the target was measured by using a laser displacement when we observed the sticking.

[Result] We classified the collisional types into 5 types according to the largest fragment mass normalized by the original target mass (m_l/M_t) and the antipodal fragment velocity (V_a); they are rebound of the projectile ($m_l/M_t \sim 1$), sticking of projectile ($m_l/M_t > 1$), cratering ($1 < m_l/M_t < 0.5$), catastrophic disruption ($m_l/M_t < 0.5$), catastrophic disruption with penetration of the projectile ($m_l/M_t < 0.5$ and $V_a \gg V_g$). As a result, it was found that sticking of projectile occurs at the target porosity larger than 60% and at the sticking velocity from 40 to 90 m/s for the porosity of 60% and from 15 to 70 m/s for the porosity of 70%. The depth of a crater hole formed by sticking of projectile was measured to find that the penetration depth was nearly proportional to the impact velocity and that the depth formed on the target with the porosity of 70% was 5 times deeper than that of 60% target at the same velocity. The penetration depth derived at the impact condition of Q^* was 1/6 of the target length for 60% and 1/2 of the target length for 70%.

[1] Wurm and Blum (1998), *Icarus* 132, 125-136. [2] Wada et al. (2009) *APJ* 702, 1490-1501. [3] Wada et al. (2010) Clarification of collision physics of planetary bodies (VI)

Keywords: impact experiment, icy planetesimal, porosity, sticking, penetration

PPS020-20

Room:103

Time:May 24 15:30-15:45

Effects of medium filling pores on impact disruption of rubble-pile bodies

Yukihiro Fujita^{1*}, Masahiko Arakawa², Sunao Hasegawa³

¹Nagoya University, ²Graduate School of Science, Kobe Univ., ³Japan Aerospace Exploration Agency

Introduction

Rubble-pile bodies could be constructed from collisional fragments and these fragments were re-accumulated by mutual gravitational force. It is expected that rubble pile bodies have large macro porosity with the size of the same order of the constituent fragments because the fragments were accumulated randomly. According to our previous impact experiments on rubble pile bodies, we found that these macro pores caused the attenuation of the impact pressure drastically and, therefore, the rubble-pile structure was quite efficient to prevent impact disruption of the constituent fragments. Furthermore, these macro pores might be filled with solid medium, such as regolith and dusts, actually. The medium filling the pores among the fragments would surely affect the impact disruption. Thus, we performed high-velocity impact experiments on rubble pile targets to investigate the effect of medium filling the pores on impact disruption.

Experimental methods

We used 1/4-inch Nylon spheres for the projectile and it was launched by a two-stage light gas gun. These projectiles were impacted on cylindrical targets at the velocity ranging from 2~7km/s. These targets are made of 7mm glass beads and the pore spaces were filled with gypsum or ice. Impact fragmentation was observed by a high-speed video camera with the framing rate of 10000~125000 frames sec⁻¹ and the fragment velocities were analyzed for each shot. Additionally, we recovered these fragments after the shot and estimated the impact damage of the target

Experimental results and discussions

We proposed M_{fsum} as a new parameter to describe the impact damage of rubble-pile targets, quantitatively. M_{fsum} is defined to be the total mass of fragments whose mass is less than a half mass of the original bead. We compared the impact damage of the targets whose pore spaces filled with gypsum or ice with that of the target without medium. As a result, M_{fsum} obtained from the targets with medium was found to be about two times larger than that without medium. Antipodal velocity observed for the target with medium also was found to be two to four times higher than that of the target without medium. Therefore, we expect that the impact disruption of rubble-pile targets could be enhanced by the medium filling the pore spaces among constituent fragments. Furthermore, the degree of disruption of rubble pile targets might be controlled by the physical properties of the medium.

Keywords: rubble-pile bodies, impact disruption, minor body, planetesimals, re-accumulation, attenuation of impact pressure

Japan Geoscience Union Meeting 2011

(May 22-27 2011 at Makuhari, Chiba, Japan)

©2011. Japan Geoscience Union. All Rights Reserved.



PPS020-21

Room:103

Time:May 24 15:45-16:00

Highvelocity impact flashes by porous impactors II

Masahisa Yanagisawa^{1*}, Ryosuke Ebina¹, Yuta Takahashi¹, Sunao Hasegawa²

¹Univ. Electro-Communications, ²Japan Aerospace Exploration Agency

Impacts at velocities of several km/s generate luminous flashes. The visible luminous efficiencies (or optical efficiencies) are defined as the ratio of the luminous energy in the visible wavelengths to the impact energy (kinetic energy of projectile). We obtained the visible luminous efficiencies in laboratory experiments in the two stage light gas gun facility in ISAS/JAXA. Spherical nylon projectiles of 7 mm in diameter were shot at tiny targets of about 1 mm in size. The tiny targets are made of solid nylon or porous nylon. The experiments are approximately equivalent to the impacts of these tiny impactors onto semi-infinite plane of nylon. Thus, we can compare the luminous efficiencies, between the impacts of solid and porous impactors, onto semi-infinite plane. The experimental results show that the efficiency for the porous impactors could be larger than that for the solid impactors.

This research was supported by JSPS KAKENHI (19540443), and the Space Plasma Laboratory, ISAS/JAXA.

Keywords: high velocity impact, impact flash, Lunar impact flash

PPS020-22

Room:103

Time:May 24 16:00-16:15

Observation of Spallation Phenomena in Hypersonic Wind Tunnel Experiment Simulating Atmospheric Entry of Icy Object

Kojiro Suzuki^{1*}, Osamu Imamura², Takeo Okunuki²

¹Dept. Advanced Energy, GSFS, Univ. Tokyo, ²Dept. Aero and Astronautics, Univ. Tokyo

The hypersonic wind tunnel, which has been used for the research and development of high speed aircrafts and spacecrafts in the aerospace engineering, is also a useful tool to simulate the flowfield around an atmospheric entry object, such as a meteorite, and to observe the various phenomena induced by the flow (Suzuki, et al., JpGU Meeting 2010, PPS004-10, Imamura, et al., AIAA Paper 2010-4512). In this paper, we present the spallation phenomena observed in the wind tunnel experiment using an ice piece. The experiments have been conducted at the hypersonic and high-enthalpy wind tunnel (http://daedalus.k.u-tokyo.ac.jp/wt/wt_index.htm) in Graduate School of Frontier Sciences, the University of Tokyo. In this facility, the uniform flow at Mach number 7.0-7.1 is obtained in the region of about 120mm diameter around the tunnel axis for 60s at maximum. Assuming an icy object entering the atmosphere, we prepare the test piece of a 40mm-diameter sphere made from water ice around the 15mm-diameter spherical core made from acrylic resin or foam aluminum. The ice piece is set in the test section by the supporting rod via thermal insulator (bakelite rod) and is injected into the test section after the uniform flow has been established.

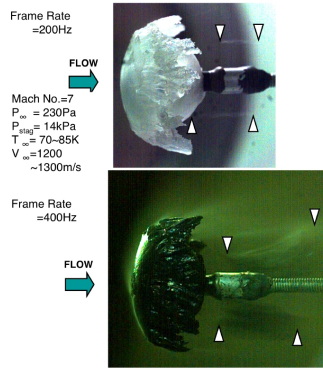
The attached figure shows the snapshots taken by the high-speed camera at about 25s from the injection into the flow. The frame rate is 200Hz and 400Hz for the upper and lower images, respectively. In both cases, the pressure and heating rate at the stagnation point on the surface are estimated as about 14kPa and 100kW/m², respectively. The maximum temperature of the flow is 800-920K. In the case of the lower picture, the test piece is made from black water dyed with Indian ink (5% wt.). In the stagnation region, the recession of the surface occurs by the melting and/or evaporation under the severe aerodynamic heating. The liquid water and vapor go downstream and are refrozen into ice due to the temperature decrease at the rapid expansion flow in the shoulder region. The pile of icy columns grows outward, forming a brim-like shape around the icy body. In the upper image, we successfully captured the spallation, in which very small icy pieces are ejected from tips of frost-like icy columns. The triangular symbols in the image indicate the beginning and end points of a streak of a spalled particle during the exposure time of the camera (5ms). In this case, the ejection velocity is estimated as in the order of 1-10m/s from the length of a streak. However, there are a variety of the streak shape and length. This means that the ejection speed and trajectory of the spalled particle are not uniform.

The high-speed video image shows that such spallation frequently occurs after the pile of the icy columns has been constructed. The mass loss due to the spallation is not negligible in comparison with that by the evaporation at the surface. At the tip of the icy column, the detailed shape looks similar to the frost. The size of the spalled particle is in the same order of the scale of the frost-like shape, which is much smaller than the size of the icy object. In the similar way, a large amount of small spalled particles are expected to be ejected into the wake flow of a meteorite.

The pile of icy columns in the shoulder region remains by the balance of the refreezing and spallation. After long exposure time, the breakup of a icy column occurs at some timing. The lower image shows the snapshot of the test piece just after the breakup, where the light scattering is observed due to a large amount of mist injected from cracks on the ice.

Such simulation experiments using a hypersonic wind tunnel are expected to provide useful information for understanding the phenomena of an atmospheric entry object such as meteorite.

This work is supported by Grant-in-Aid for Scientific Research (B) No. 21360413 of Japan Society for the Promotion of Science.



Keywords: atmospheric entry, ice, ablation, spallation, hypersonic flow, wind tunnel experiment

PPS020-23

Room:103

Time:May 24 16:30-16:45

Observations of Internal State in Oblique-Impact-Induced Vapor Clouds

Taiga Hamura^{1*}, Kosuke Kurosawa¹, Sunao Hasegawa², Takafumi Matsui³, Seiji Sugita¹

¹Dept. of Complexity Sci. and Eng., Univ., ²ISAS/JAXA, ³PERC, Chiba. Inst. of Tech.

Organic supply processes on prebiotic Earth are thought to be contributed by chemical synthesis in the atmosphere, exogenic delivery via cometary/asteroidal impacts, and in situ production driven by impacts (Chyba and Sagan, 1992). Because organic synthesis process due to impacts occurs in limited periods of time and limited spatial extents, it would lead to a higher concentration of organics for a given total amount of organic supply and higher efficiency of sequent chemical reactions. Previous experiments show that most organics originally contained in meteorites are decomposed by intense shock heating at near-vertical impact angles (Mukhin et al., 1989). In the case of oblique impacts, it was suggested that the most organics also decomposed by intense aerodynamic heating during the downrange drifting (Sugita and Schultz, 2003a). Low-angle impact experiments using polycarbonate projectile within a nitrogen atmosphere, however, show that CN is formed efficiently from reduced carbon supplied from the projectiles and nitrogen in the atmosphere (Sugita and Schultz, 2009). However, there are neither time-series nor spatially-imaged detail observations of the interior thermochemical state of the vapor cloud. Therefore, the details of physical and chemical reaction within the vapor cloud, the distributions of compositional gas and fragment, and the region for chemical reaction with ambient atmosphere are still unknown. {cr/}

Thus, we performed the oblique impact experiments with a two-stage light gas gun at ISAS. Projectile, impact velocity, impact angle, and ambient pressure of nitrogen atmosphere are polycarbonate spheres (7 mm in diameter), 4.8-6.5 km/s, 30 degree from the horizontal, and 30 hPa, respectively. We observed the motion of self-luminous vapor clouds and gas/fragments distribution in the clouds using two high-speed cameras of framing rate at 2 us/frame with different band-pass filters. Transmission wavelength ranges of the band pass filters are 373 nm to 387 nm (CN), 400 nm to 410 nm (Blackbody) and 505 nm to 515 nm(C_{2}^{2}). A high-speed time-series spectrometer observed to measure time variation of spectrum and blackbody temperature of fragments in the vapor cloud. {cr/}

Thus, we revealed the spatial difference among distributions of projectile fragments and gas components. These three components are sequentially distributed; projectile fragment, C_{2}^{2} gas, and CN gas from the top to the back of the vapor cloud. The sequence suggests a scenario that the gas decomposed of projectile fragments within the top of the vapor cloud is flowed down with wake flow, and chemically changed to CN radical within the back of the vapor cloud. In addition, we measured the transitional velocity of the horizontally drifting vapor cloud which almost keeps its shape during its motion. First, instant acceleration of vapor cloud to 1.9 times the impact velocity is seen. Then it decelerates to the degree of impact velocity during almost 25 us due to air resistance. Additionally, we solved the equation of motion of the vapor cloud to analyze its motion. Because the measured vapor velocity is well explained when it was assumed constant mass and cross-section toward drifting direction, it was indicated that mass concentrated locally in the cloud.

Measured temperature is achieved to 5000 K at 10 us after impact when the vapor came into the field of view of the spectrometer, then it fell down to 2500 K at 45 us after the impact. Vaporization rate is estimated from the temperature and measured velocity based on heat balance on fragment surface. It is higher than Sugita and Schultz (2003b). The primary reason of such a difference is that they assume the downrange velocity of impact vapor clouds to be approximately the same as the horizontal component of the impact velocity, which is only about the half the actual value as revealed by the high-speed imaging observation in this study.

Keywords: impact, organic resynthesis, impact vapor cloud, aerodynamic heating

PPS020-24

Room:103

Time:May 24 16:45-17:00

Gas-phase chemical analysis in an open system using a 2-stage light gas gun: HCN production due to small-scale impacts

Kosuke Kurosawa^{1*}, Sunao Hasegawa², Tetsu Mieno³, Sohsuke Ohno⁴, Takafumi Matsui⁴, Seiji Sugita¹

¹The Univ. of Tokyo, ²ISAS/JAXA, ³Shizuoka University, ⁴Chiba Institute of Technology

Hydrogen cyanide (HCN) is one of the most important molecules in the origin of life. Amino acids and Nucleic acid basis can be produced from concentrated solution of HCN. We focus on HCN production by meteoritic impacts because the impact-induced HCN is concentrated into a narrow region and produced within a very short period of time.

The geologic record of the Moon investigated by the Apollo Project show that impact flux on the Earth at 3.8 ? 4.0 Gyr ago is ~10³ times higher than that on the present Earth (late heavy bombardment period). In this period, the influx of both materials and energy into the Earth may have been the largest in its history. Such intense bombardment may have controlled the evolution of surface environments on the early Earth. Our goal is to investigate the production efficiency of HCN due to hypervelocity impacts and to understand the role of meteoritic impacts on the origin of life on the early Earth.

We are developing the experimental method to reproduce hypervelocity impacts in the early Earth atmosphere using a 2-stage light gas gun at JAXA. As a first step, we developed the experimental procedure of gas-phase chemical analysis in an open system. In previous studies with 2-stage light gas guns, chemical analyses were usually conducted in closed systems using containers to pretend the chemical contamination by gunpowder. In this case, thermodynamic path of shock-heated material, however, is different from natural impacts. To conduct chemical analysis in an open system, we set a large-volume chamber, an air-driven automatic gate valve, and an Al diaphragm to uprange of an experimental chamber to prevent intrusion of contaminant gas into the chamber. In this study, we used polycarbonate, polystyrene, and N₂ gas as projectiles, targets, and atmospheres respectively. The total pressure in the chamber was fixed at 105 Pa. The impact velocity was fixed at 6.5 km/s. After the shoot, we measured the final gas phase products in the chamber using a detecting tube for HCN. We successfully detected HCN with molar concentration of ~50 ppm. We roughly estimated the conversion efficiency from vaporized carbon to gaseous HCN as ~0.1%.

For the future works, we are planning to a series of hypervelocity impact experiments using actual meteoritic materials and simulated early Earth atmospheres. The developed procedure can be widely used for impact-induced degassing phenomena.

Keywords: Hypervelocity impacts, Chemical gas-phase analysis in an open system, 2-stage light gas gun, Hydrogen cyanide, The origin of life, Impact degassing

PPS020-25

Room:103

Time:May 24 17:00-17:15

Recovery experiment of high-power laser shock compressed olivine and Application to Planetary Science

Keita Nagaki^{1*}, Tatsuhiko Sakaiya¹, Tadashi Kondo¹, Toshihiko Kadono², Yoichiro Hironaka², Keisuke Shigemori²

¹Graduate School of Science, Osaka Univ, ²Institute of Laser Engineering, Osaka

It is important to recover the shock-compressed samples for understanding the synthetic mechanism of high-pressure phase, shock metamorphism and shock-melt vein in meteorites. In the past, many impact experiments have conducted by using explosive or gas guns. In fact, although high-pressure phase in meteorites is recovered by the impact experiments (the impact velocity is 1.5km/s and the impact pressure is 26GPa) [1], the impact velocity in these methods is limited below 10km/s less than second escape velocity on the Earth. Recently, impact experiments at the velocity over 10km/s were conducted by using projectiles which were accelerated by high-power laser [2]. In previous experiments on the laser-shocked compression, the samples were recovered on the pressure below 100GPa (the olivine which is samples in this experiment is molten at the pressure of 150GPa).

We developed the recovery technique of the laser-shocked materials at higher pressure (at 200-300GPa in this experiments) by high-power laser system and analyzed the pressure range of the production conditions from the structure of shock metamorphism. We used the single crystal olivine (from San Carlos, USA) which is a major mineral of meteorites and the mantle of the Earth. We used GXII/HIPER laser system at Institute of Laser Engineering, Osaka University [3]. The deformation, fracture and phase identification of the recovered olivine were observed comprehensively by optical microscopy, field emission-scanning electron microscopy, electron backscatter diffraction and micro-Raman spectroscopy.

We designed the new recovery cell. In this cell, Ti plate was put in front of olivine to prevent the sample from blowing off. We could recover 100wt% of the sample by using this cell. In the recovered sample, there are the region of some distinctive structures. We will report the detail of the recovery technique and the results of the observation of the recovered samples.

References

- [1]Tschauer, O. et al., Proceedings of the National Academy of Sciences, 106, 13691-13695, 2009
- [2]Kadono, T. et al., Journal of Geophysical Research, 115, E04003, 2010.
- [3]Yamanaka, C. et al., Nucl. Fusion, 27, 19-30, 1987.

PPS020-26

Room:103

Time:May 24 17:15-17:30

Development of a laser ablation isochron K-Ar dating method for landing planetary missions

Yuichiro Cho^{1*}, Yayoi N. Miura¹, Seiji Sugita²

¹Earth and Planetary Science, Univ. Tokyo, ²Complexity Sci. and Eng., Univ. Tokyo

Absolute age measurements of planetary surfaces are extremely important for understanding the evolution of planets. However, no chronological measurements of planetary materials with known geological contexts have been made except for the lunar samples. Although the absolute age estimates for Martian surfaces have been proposed on the basis of the lunar chronology and the orbital calculations of asteroids, there still remain uncertainties as large as 1 billion years. If the absolute ages of rock samples from a geologic unit, where crater number density is known, are determined down to around 10% accuracy, it will make a significant contribution to understandings of the evolution of Mars.

In this study, we developed a new in-situ dating method based on the Potassium-Argon (K-Ar) dating technique toward future landing planetary missions. We propose a simpler and more accurate in-situ K-Ar dating method than those employed in previous mission plans, using laser-induced breakdown spectroscopy (LIBS) and a quadrupole mass spectrometer (QMS). We conducted the following experiments to evaluate the feasibility of the K-Ar dating with the LIBS-QMS method.

In the first part of this study, we measured K abundance using LIBS. First, we irradiated laser pulses on 13 samples with 100 ppm to 5 wt% of K₂O and observed the emission lines of K from these samples. We obtained two calibration curves from K emission lines at 766.49 nm and 769.89 nm. Our results show that K concentration can be quantified within the relative accuracy of 10% for 2000 ppm to 5 wt% range. The detection limit was 1000 ppm.

Second, the volumes of laser-ablated craters on rock samples are measured with a microscope. The observations indicate that the crater volumes of basaltic rocks are within the uncertainty of 11% except for some minerals such as olivine. When these results are combined, the absolute abundance of K inside a crater is estimated within the accuracy of 15%.

In the second part of this study, we built a new Ar experimental system optimized for K-Ar dating, based on experimental results from a previously established system. As a first step, we used the previously established gas analytical system to estimate the detection limits and the pulse numbers required to the K-Ar dating. We estimated $40\text{Ar}=10^{-12}$ cc/pulse and $36\text{Ar}=10^{-15}$ cc/pulse are released from desirable Martian rocks. The blank levels for the system were 5×10^{-10} cc and 1×10^{-10} cc at $m/Z = 40$ and 36 , respectively, and the electric noise level was 1×10^{-11} cc. These blank levels should be 10-100 times lower in order to detect Ar from the rocks within 1000 laser pulses.

A measurement of the blank using the new gas analysis system indicates that the detection limit of 40 and 36 and electrical noise of the detector are on the order of 10^{-11} cc, less than 10^{-11} cc and less than 10^{-11} cc, respectively. This is an improvement by one order of magnitude compared with our former experimental system. These results indicate that a sufficient amount of 36Ar can be evaporated by 1000 laser pulses on the Martian rocks.

These experimental results using our breadboard model strongly suggests that an experimental system that can simultaneously measure K and Ar released from the same laser-vaporized mass of a sample can be built with currently commercially available parts. Thus, the new K-Ar measurement method proposed in this study using a pulse laser, a spectrometer and quadrupole mass spectrometer is a viable candidate for an on-board instrument for a future Mars landing mission.

Keywords: Chronology, LIBS, QMS, Planetary exploration

Japan Geoscience Union Meeting 2011

(May 22-27 2011 at Makuhari, Chiba, Japan)

©2011. Japan Geoscience Union. All Rights Reserved.



PPS020-27

Room:103

Time:May 24 17:30-17:45

Remote sensing observations of Hayabusa2: Linking ground-based observations and the returned sample analysis

Ryosuke Nakamura^{1*}, Naru Hirata²

¹AIST, ²University of Aizu

Hayabusa-2 is the second Japanese sample return mission from a C-type asteroid 1999JU3. In this presentation, we introduce the specification and operation plan of the four nominal onboard remote-sensing instruments, i.e. Asteroid Multi-band Imaging Camera (AMICA), LIDAR, Near-Infrared spectrometer (NIRS3) and Thermal InfraRed Imager (TIR). The in-situ observations will provide the geological context of the returned sample. We expect to link the global structure of asteroid belt revealed by ground-based telescopic observations and detailed analysis of returned sample from a specific asteroid through remote-sensing by Hayabusa-2 spacecraft.

Keywords: remote sensing, asteroid, Hayabusa2, sample return, camera

An attempt to estimate the stability of Jupiter's atmosphere based on the vertical structure of large-scale disturbances

Shoji Kawashita^{1*}, Kensuke Nakajima²

¹Graduate School of Sciences, Kyushu Univ, ²Faculty of Sciences, Kyushu Univ

1. introduction

The vertical structure of Jupiter's atmosphere, namely the composition in far below the visible cloud, remains as an unresolved issue presently, because the only direct observation, which is done by the Galileo Probe in 1995, presumably did not succeed in obtaining the global properties. Thermodynamics calculations (e.g., Weidenschilling and Lewis, 1973; Sugiyama et al. 2006) can estimate the atmospheric structure once a hypothetical composition in the deep levels is employed, but the results must be verified by observation.

Allison (1990) argued that the large-scale disturbances observed in the North Equatorial Belt may serve as a clue. Stratospheric temperature profiles obtained by the Voyager radio occultation suggest the existence of vertically propagating waves (Lindal et al. 1981). Assuming that the waves are equatorial Rossby waves, Allison(1990) compared the vertical wavelength of the observed waves and that of the vertical eigenmodes of a simplified atmosphere consisting of 4 layers, one of which is cloud layer, and estimated the thickness and stability of the cloud layer. In this study, we generalize the approach of Allison so that we can consider more complex atmospheric structure and try to estimate the deep atmospheric composition.

2. Method

We numerically solve the vertical structure equation as a forced problem and search the values of the equivalent depths at which the response in the stratosphere become resonantly large, and compare those values with the equivalent depth of the vertically propagating waves found by the radio occultation. We employ three types of the atmospheric structure, which are based on the Jupiter's atmospheric static stability profiles with solar, 5 times solar and 10 times solar abundance of condensable components obtained by Sugiyama et al.(2006). The forcing is a vertically localized layer of heating in the water cloud level.

3. Results

We found a set of discrete values of equivalent depths that are related to the resonant excitation with all of the three atmospheric profiles. The value of the equivalent depth of the first mode, which is the largest equivalent depth of resonance, is 0.4km, 1.9km, and 3.9km for solar, 5 times solar and 10 times solar abundance of condensable components, respectively. The waves found in Lindal et al (1981) has the equivalent depth of 2.2km (Allison,1990) and is explained best with 5 times solar abundance of condensable gasses.

Keywords: Jupiter's Atmosphere

PPS020-29

Room:103

Time:May 24 18:00-18:15

Numerical experiments of synchronously rotating planets with increasing solar constant

Satoshi Noda^{1*}, Masaki Ishiwatari², Kensuke Nakajima³, Yoshiyuki O. Takahashi⁴, Yasuhiro MORIKAWA⁵, Seiya Nishizawa⁴, Yoshi-Yuki Hayashi¹

¹Kobe University, ²Hokkaido University, ³Kyushu University, ⁴Center for Planetary Science, ⁵NICT

Many exoplanets orbit nearby central stars and are thought as synchronously rotating planets because of the strong tidal force of the star. In the vicinity of small and low luminous stars such as M dwarfs, there may exist synchronously rotating terrestrial planets with liquid water on their surface.

In order to investigate the climate of synchronously rotating planets, we have performed numerical experiments with various rotation rate and solar constant fixed at Earth's value. These experiments showed that, according to rotation rate, there existed several climate regimes: equilibrium states in which a direct circulation from day side to night side dominate, equilibrium states in which disturbances with precipitation and equatorial waves dominate, and so on.

However, for increased solar constant, the atmosphere cannot reach equilibrium states and the runaway greenhouse state appears. In these cases, liquid water cannot exist on the planetary surface. In this study, for the purpose of examining the dependence of threshold values of solar constant at which the runaway greenhouse occurs (hereafter, "runaway limit") on planetary rotation rate, we perform numerical experiments with varying the values of solar constant and planetary rotation rate.

The model utilized here is atmospheric general circulation model, dcpam5 (<http://www.gfd-dennou.org/library/dcpam/index.htm.en>). The atmosphere consists of the dry air (noncondensable component) and vapor (condensable component).

The radiative processes are quite crude. Shortwave radiation is not absorbed by the atmosphere, while longwave radiation is absorbed only by vapor. We assume no scattering by cloud. Moist convective adjustment (Manabe et al., 1965) is used to include effects of cumulus convection.

The surface is assumed to be covered with swamp (zero heat capacity wet surface) and surface albedo is zero. The values of radius and surface pressure are the same as those of the Earth.

We use two types of the insolation pattern. One is the synchronously rotating condition (SR) in which the subsolar point is fixed to a point on the equator. Another is the annual and diurnal mean insolation pattern of the Earth (nonSR). The values of rotation rate we examine are zero and same value of the Earth. In the experiment with these two rotation rates

and solar constant of Earth's values, we have obtained different equilibrium states. In this study, five values of solar constant are used:

from the Earth's value to increased values. All experiments consist of 18 cases (see table).

The resolution used in this study is 5.6 degrees longitude-latitude grid with 48 vertical layers. The model is integrated for 2000 Earth days from isothermal atmosphere at rest.

Results of experiments show that equilibrium state is not reached in all cases with solar constant of 1600 W/m². In these cases, global mean outgoing longwave radiation flux decreases monotonically with time, while global mean surface temperature increases monotonically. It is considered that the runaway greenhouse state occurs in these cases.

The value of the runaway limit tends to increase with decreasing the rotation rate of the planet. On the other hand, for same values of rotation rate, the runaway limit in nonSR case is larger than that in SR case.

Run summaries in each insolation pattern('Pattern', 'SR' represents synchronously rotating condition, and 'nonSR' represents the Earth like condition), rotation rate(Ω , normalized by the Earth's value), solar constant(S , W/m²). Circles represent the atmosphere reaches equilibrium state, while crosses represent the atmosphere does not reach equilibrium state. blank is not calculated.

Pattern	SR		nonSR	
$S \setminus \Omega$	0	1	0	1
1600	×	×	×	×
1550	×	×	○	×
1500	○	×	○	○
1450	○	○		
1380	○	○	○	○

Keywords: synchronously rotating planet, general circulation model, exoplanet, runaway greenhouse state, solar constant

Japan Geoscience Union Meeting 2011

(May 22-27 2011 at Makuhari, Chiba, Japan)

©2011. Japan Geoscience Union. All Rights Reserved.



PPS020-30

Room:103

Time:May 24 18:15-18:30

SPICA Coronagraph Instrument (SCI) and study of exoplanets

Keigo Enya^{1*}, the SCI team¹

¹Japan Aerospace Exploration Agency

We present Space Infrared telescope for Cosmology and Astrophysics (SPICA),

SPICA Coronagraph Instrument (SCI), and observation of exoplanets with them. SPICA is an international mission led by JAXA with contribution of ESA and others. The launch of SPICA is planned in 2018. SPICA will have 3m class telescope and whole of it will be cooled to 6K to realize high sensitivity and special resolution. In various scientific objective of SPICA, one of the most important target of SPICA is detail observation of exoplanets. SCI is a specially designed instrument for the high contrast observation of exoplanets. SCI is expected to provide unique data for the study of exoplanets, not only detection but a catalogue of spectrum of Jovian exoplanets. Monitor observation of transiting planets, imaging and spectroscopy of circumstellar discs are also important target of SCI. Observation of diversity of exoplanets with SPICA is complementally with detail study of the solar system planets.

Keywords: SPICA, coronagraph, SCI, exoplanet, infrared, transit